Science of the Total Environment 603–604 (2017) 390–400

Contents lists available at ScienceDirect

Science of the Total Environment

journal homepage: www.elsevier.com/locate/scitotenv

Spatial and temporal variation in autochthonous and allochthonous contributors to increased organic carbon and nitrogen burial in a plateau lake

Changchun Huang [a,b,c,d,*], Ling Yao [e], Yunlin Zhang [f], Tao Huang [a,d], Mingli Zhang [a], A-Xing Zhu [a,c,g], Hao Yang [a,d]

[a] Jiangsu Center for Collaborative Innovation in Geographical Information Resource Development and Application, Nanjing Normal University, Nanjing 210023, China
[b] State Key Laboratory of Lake Science and Environment, Nanjing Institute of Geography and Limnology, Chinese Academy of Sciences, Nanjing 210023, China
[c] Key Laboratory of Virtual Geographic Environment (Nanjing Normal University), Ministry of Education, Nanjing 210023, China
[d] School of Geography Science, Nanjing Normal University, Nanjing 210023, China
[e] State Key Laboratory of Resources and Environmental Information System, Institute of Geographic Sciences and Natural Resources Research, Chinese Academy of Sciences, China
[f] Nanjing Institute of Geography and Limnology, Chinese Academy of Sciences, Nanjing 210023, China
[g] Department of Geography, University of Wisconsin, Madison, WI 53706, USA

HIGHLIGHTS

- Quantitatively evaluate the contribution of autochthonous and allochthonous source to the increased OCAR and ONAR.
- Developed a multi-source mixing model based biomarkers, n-alkanes, to distinguish the autochthonous and allochthonous source.
- Fill gaps in the study of Organic-C and -N accumulation in the freshwater plateau lake.

GRAPHICAL ABSTRACT

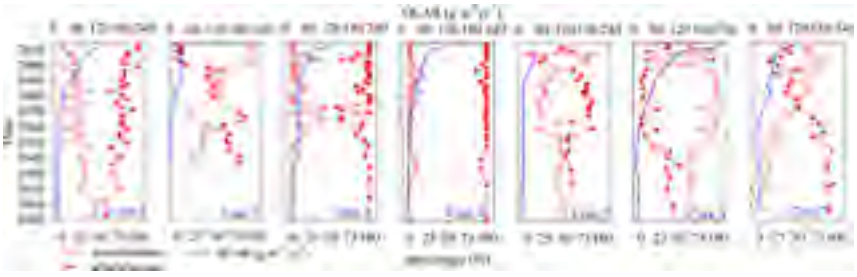

ARTICLE INFO

Article history:
Received 5 April 2017
Received in revised form 24 May 2017
Accepted 14 June 2017
Available online xxxx

Editor: Elena Paoletti

Keywords:
Dianchi Lake
Algal blooms
Human activities
Carbon cycling
Land-use cover change

ABSTRACT

Increased organic carbon and nitrogen accumulation rates (OCAR and ONAR) in lake sediment significantly regulate the global carbon cycle. However, the reasons for and contributors to the increased OCAR and ONAR are unclear. Seven sediment cores, collected in July 2014 from Dianchi Lake, China, were used to evaluate the effects of autochthonous and allochthonous sources on OCAR and ONAR. The results indicate that OCAR and ONAR increased by factors of 4.33 and 7.34 over the past hundred years (1900–2000), particularly after algal blooms began to occur frequently (beginning in the 1980s). Dianchi stored 0.467 ± 0.0055 Tg (mean value ± standard deviation) organic carbon (OC) and 0.033 ± 0.0004 Tg organic nitrogen (ON) after 1986, which is almost equal to the total storage of OC and ON from 1900 to 1985 (OC, 0.468 ± 0.0022 Tg; ON, 0.032 ± 0.0002 Tg). OCAR and ONAR increases were due to increasing autochthonous production and allochthonous loading. Examination of the increased OCAR, which was estimated from a newly developed multi-source mixing model, suggests that >90% of increased OCAR was caused by allochthonous sources (such as intensified cultivation, land-use cover change, etc.) in southern and eastern Dianchi and that >70% of the increased OCAR was due to autochthonous sources in western and northern Dianchi Lake. The significant spatial and temporal variation in the contributors to increased OCAR indicates complicated migration and transformation of OC in inland lakes. Land use cover change around Dianchi and the occurrence of algal blooms regulate the contributions of allochthonous and autochthonous sources to the increased OC and ON.

* Corresponding author at: Nanjing Normal University, Geography, Nanjing normal university K3-510, 210046 Nanjing, China
E-mail address: huangchangchun_aaa@163.com (C. Huang).

http://dx.doi.org/10.1016/j.scitotenv.2017.06.118
0048-9697/

1. Introduction

Lakes are an important carbon pool. They emit greenhouse gases and store organic carbon (OC), thus playing a pivotal role in the global carbon cycle (Cole et al., 2007). Lake sediment buries large amounts of OC and thus acts as a significant carbon sink (Tranvik et al., 2009; Buffam et al., 2011). Previous studies have globally estimated that 1.88 Pg C y^{-1} of the OC that inland water receives is derived from terrestrial ecosystems. About 48% of this carbon (0.9 Pg C y^{-1}) is transported to the ocean, while the remainder reaches the lake sediment surface (0.98 Pg C y^{-1}) and 23% (0.23 Pg C y^{-1}) is eventually buried after the process of OC mineralization (Cole et al., 2007; Tranvik et al., 2009; Buffam et al., 2011). Mineralized OC is emitted as carbon dioxide (CO_2) and methane (CH_4) via microbial activity. This emission of CO_2 and CH_4 from inland waters significantly offsets the continental carbon sink and thus affects the global carbon cycle and climate change (Johnson et al., 2008; Buffam et al., 2011; Bastviken et al., 2011; Raymond et al., 2013). The mass of emitted CO_2 and CH_4 is regulated by the composition of the organic matter, temperature, oxygen exposure and the dynamic characteristics of the lake (Stief, 2007; Gälman et al., 2008; Gudasz et al., 2010; Sobek et al., 2009, 2014; Cardoso et al., 2014). Both carbon exported from land (allochthonous) and fixed by photosynthesis in aquatic ecosystems (autochthonous) contribute to the emission of CO_2 and CH_4, but with different mineralization rates (Gudasz et al., 2012). The effects of temperature and organic composition (autochthonous/allochthonous) on OC mineralization have been widely studied, and it has been proposed that OC mineralization increases with temperature, oxygen exposure and the percentage of autochthonous product (Gudasz et al., 2010, 2012; Watanabe and Kuwae, 2015; Chmiel et al., 2015). Temperature is a conventional parameter in meteorology and has been widely monitored, but the composition of organic matter has not.

Recent studies have proposed that the accumulation rate of OC has increased significantly over the last century (Kastowski et al., 2011; Larsen et al., 2011; Dong et al., 2012; Heathcote et al., 2015). The morphology, trophic state, climate and vegetation in the watershed of lakes influence OC accumulation in sediment (Alin and Johnson, 2007; Kortelainen et al., 2013; Anderson et al., 2014; Mendonça et al., 2016; Leithold et al., 2016). Global warming has also been shown to significantly increase OC burial (Heathcote et al., 2015). This finding was not confirmed by Anderson et al. (2013), who found that land-use change is more responsible than climate change for increased OC burial in Minnesotan lakes (USA). Eutrophication, caused by the enrichment of nutrients in lake water, is known to increase primary productivity and organic carbon in lakes and has been considered as another important driver of the increasing carbon burial rate (Downing et al., 2008; Heathcote and Downing, 2012; Anderson et al., 2014). In addition to representing the composition of OC in the sediment, autochthonous and allochthonous sources also determine the contribution of exotic terrestrial materials and local primary production to increased OC burial. However, the contributions of allochthonous and autochthonous sources, which regulate the composition of organic matter in the sediment, to the increased OC have not been determined. Consequently, understanding the contributions of autochthonous primary production and allochthonous terrestrial materials to increased OC burial in lake sediment is not only critical to further understand the spatial and temporal variation of greenhouse gases emitted from sedimentary OC mineralization but also to comprehend the effects of human activities and eutrophication on the global carbon cycle.

Most previous studies have focused on boreal lakes, and some have focused on temperate-zone lakes (such as in Europe, United States, etc.) to understand the process of OC burial over different time scales, the burial efficiency of OC and influencing factors to OC burial (Kastowski et al., 2011; Heathcote and Downing, 2012; Sobek et al., 2014; Ferland et al., 2014; Anderson et al., 2013, 2014; Heathcote et al., 2015; Isidorova et al., 2016). However, OC burial and its response to eutrophication and human activities in sub-tropic plateau lakes are largely unstudied. The sub-tropic plateau lakes in our study area are impacted by a variety of climatic features, such as monsoons and highland and low-latitude climates. The temperature difference between seasons is not significant; winters are relatively warm and summers are relatively cool.

n-Alkane is one of the most abundant lipid molecules, and it widely exists in plants and algae (Giger et al., 1980; Ficken et al., 2000). The carbon number distribution of *n*-alkanes in sediment can be used to trace the source of OC (Meyers, 2003; Ortiz et al., 2011; Silva et al., 2012; Fang et al., 2014). Short-chain *n*-alkanes (n-C_{14}–n-C_{20}) suggest algae, bacteria and fungi sources (Giger et al., 1980; Meyers, 2003), especially the unimodal distribution maximizing at n-C_{17}, which suggests algae and photosynthetic bacteria sources (Meyers, 2003). Mid-chain *n*-alkanes (n-C_{20}–n-C_{25}) indicate the source is submerged macrophytes (Rao et al., 2014), while long-chain *n*-alkanes (n-C_{27}–n-C_{33}) with an odd-even preference reflect a terrestrial origin (Rao et al., 2014). Study of *n*-alkanes have identified the sources of organic matter in lake sediment (Xie et al., 2003; Xiong et al., 2010; Gao et al., 2011; Fang et al., 2014; Chen et al., 2017), and a study of Dianchi Lake, the largest freshwater plateau lake in China, may fill this gap in the study of global carbon burial.

Thus, we developed a multi-source mixing model to estimate the contributions of autochthonous and allochthonous processes to OC burial and combined *n*-alkanes with OC and organic nitrogen (ON) to accomplish the objectives of this study: 1) to trace the change in OC and ON sources and burial rates over the past hundred years and 2) to distinguish the contributions of eutrophication and direct human activities on increased OC and ON burial.

2. Material and methods

2.1. Study area

Dianchi is located on the Yungui Plateau and is the largest freshwater plateau lake in China (Fig. 1). It is hypereutrophic, and algal blooms frequently occur. The concentrations of total nitrogen (TN) and phosphorus (TP) rose from 1.15 mg/L and 0.132 mg/L to 2.53 mg/L and 0.173 mg/L, respectively, from 1980 to 2010 (Zhou et al., 2016). The annual mean water temperature of Dianchi is 16 °C, and the mean depth and area are 5 m and 300 km^2, respectively. The land-use categories in the lake basin (area 2800 km^2) are mainly forest (35.71%), agriculture (22.95%) and developed land (28.55%, includes urban, residential, road and other developed land area), according to classification results from 2013 Landsat satellite imagery (Fig. 1). Dianchi is a fault depression lake. Almost all of the watershed is to the north, east and south. The Haikouzi River (blue arrow in Fig. 1) is the only outlet of Dianchi. The largest flower-producing area of Asia is located on the eastern shore of Dianchi Lake.

2.2. Methodology

2.2.1. Sampling strategy and measurement of carbon and nitrogen

Seven sediment cores were collected using a gravity-type columnar sediment sampler in July 2014. In order to reveal the spatial and temporal variation of impact factors on the increased OC and ON, these sediment cores were mainly taken from northern, eastern and southern Dianchi Lake, approximately 1 km offshore from the mouths of inflowing rivers. The sediment cores were cut into 1 cm slices and ground after being dried in a lyophilizer. Two sub-samples of 0.2 g from each ground sediment sample were used to measure the concentrations of total carbon (TC) and inorganic carbon (IC) with a TOC analyzer (Shimadzu Corp., Japan). The total organic carbon (TOC) concentration was obtained by subtracting IC from TC. Sub-samples (0.02 g) were digested by persulfate ($K_2S_2O_8$ + NaOH) at 121 °C, and total nitrogen (TN) was determined using a UV-3600

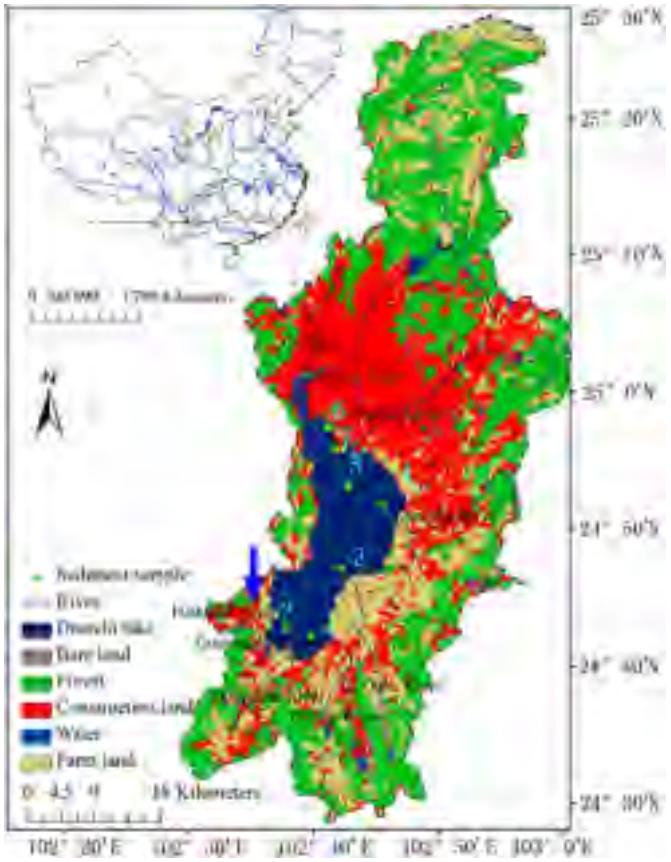

Fig. 1. Study area and sediment sampling sites. The land use of Dianchi Basin in 2013 was classified by Landsat satellite imagery. The red cross on the map of China (top left corner) shows the location. (For interpretation of the references to colour in this figure legend, the reader is referred to the web version of this article.)

spectrophotometer (Shimadzu Corp., Japan). Sub-samples of 1 g were dissolved with a potassium chloride solution. The supernatants were treated with sodium nitroprusside and hypochlorous acid to determine the ammonia nitrogen (NH_4-N) concentration, and HCl was used to determine the nitrate-nitrogen (NO_3-N) concentration, using a UV-3600 spectrophotometer (Shimadzu Corp., Japan) after pre-treatment. Total organic nitrogen was obtained by subtracting NH_4-N and NO_3-N from TN (Qian et al., 1990; Lu, 1999).

2.2.2. n-Alkane extraction

The n-alkanes were obtained via microwave-assisted extraction (100 °C, 10 min) from sub-samples (2 g), using a dichloromethane–methanol mixture (93:7, v:v). The supernatants were concentrated to 1 ml by rotary evaporation at 40 °C after three centrifugations. The concentrated supernatants were purified and separated using solid-phase extraction (Rtx® ~5MS, 30 m × 0.32 mm × 0.25 μm) and n-hexane, and then the eluent with n-alkanes was concentrated to 1 ml. The n-alkanes were quantified by measuring the concentrated eluent via gas chromatography mass spectrometry (GC/MS-QP2010 Ultra, Shimadzu Corp., Japan). The injection port temperature rose gradually to 300 °C at 10 °C min^{-1}, starting at 50 °C (Gao et al., 2011; Liu and Liu, 2016).

2.2.3. Dating and accumulation rates of OC and ON

The ground sediment sample (10 g) was sealed for a month to keep the ^{226}Ra and ^{210}Pb in radioactive equilibrium. The activities of ^{226}Ra and ^{210}Pb were measured using a high- resolution HPGe γ-spectrometer (EG&GORTEC, GWL-120-15, USA) with 62% relative detection efficiency and under 40,000 s determination time. The activity of excess ^{210}Pb ($^{210}Pb_{ex}$) is the difference between ^{226}Ra and ^{210}Pb. $^{210}Pb_{ex}$ was then used to date the sediment cores using the constant rate of ^{210}Pb supply (CRS) model (Eq. (1)), which has been widely used to estimate the geochronology of lake sediment and provides the best dating results (Appleby, 2008; Sanchez-Cabeza and Ruiz-Fernández, 2012).

$$t = \frac{1}{\lambda} \ln\left(\frac{A_h}{A_0}\right), \tag{1}$$

where λ is the decay constant of ^{210}Pb, A_h is the content of $^{210}Pb_{ex}$ at each sediment depth, and A_0 is the total content of ^{210}Pb in the sediment core. The accumulation rate of sediment mass (Sr, g cm^{-2} yr^{-1}) was calculated as

$$Sr = \frac{\partial Md}{\partial t} = \frac{\rho \cdot \partial Z/\partial t}{\partial t}, \tag{2}$$

where Md is the mass depth (g cm^{-2}), t is time (years), Z is depth (cm), and ρ is the dry bulk density (g cm^{-3}). The accumulation rates of organic carbon (OCAR) and nitrogen (ONAR) (g m^{-2} yr^{-1}) were estimated by

$$CAR\ (NAR) = Sr * \delta^* 10, \tag{3}$$

where δ is the concentration of organic carbon and nitrogen (mg g^{-1}).

2.2.4. Auxiliary data presentation

Socio-economic data about the population, gross domestic product and fertilizer consumption in the basin was collected from the National Bureau of Statistics (http://data.cnki.net/) and Gao et al. (2015a, 2015b). Temperature and rainfall data were downloaded from the China meteorological data sharing service system (http://cdc.cma.gov.cn/). The areas of each land-use type were extracted from Landsat image data by the SVM (support vector machine) classification algorithm in ENVI 5.0 Feature Extraction Module (Huang et al., 2014). The concentrations of nutrients (total nitrogen, ammonia nitrogen and total phosphorus) in water were collected from our in-situ measurements (He et al., 2015; Zhou et al., 2016).

2.2.5. Elasticity analysis model (STIRPAT model)

The stochastic model (STIRPAT) proposed by Dietz and Rosa (1994) can be used to statistically evaluate the non-monotonic or non-proportional impacts of driving factors on the environment. The STIRPAT model was used to statistically assess the effects of demographic, economic, technologic and other factors on the environment (York et al., 2003). The STIRPAT model is a stochastic model, and the impact factors can be expanded if these factors have a logical correlation to environment (Wang et al., 2013; Liu et al., 2015). STIRPAT can be written as $I_{it} = \alpha \prod (F_{it}^{a_{it}}) \varepsilon_{it}$. After taking logarithms, this equation can be written as.

$$\ln(I_{it}) = \alpha + \sum a_{it} \ln(F_{it}) + \varepsilon_{it}, \tag{4}$$

where F_{it} indicates the ith factor at time t (e.g., temperature, population, rainfall); α is a constant term; ε_{it} is the error term; and a_{it} is the elasticity coefficient with 95% confidence interval (this is the estimation result in Fig. 11). All the parameters can be estimated by multiple linear regression (Zhou et al., 2015; Zhou and Liu, 2016).

2.2.6. Source identification from n-alkanes

The mass balance equation, where the total *n*-alkane concentration in the sediment ($C_{n\text{-Alkanes}}$) is composed of all carbon chains of *n*-alkanes ($C\text{-}g_{n\text{-Alkanes}}$), was used to establish a multi-source mixing model. This model can be expressed as.

$$C\text{-}m_{n\text{-Alkanes}} = \sum_{i=1}^{n} (C\text{-}g_{n\text{-Alkanes}} \times p_i), \tag{5}$$

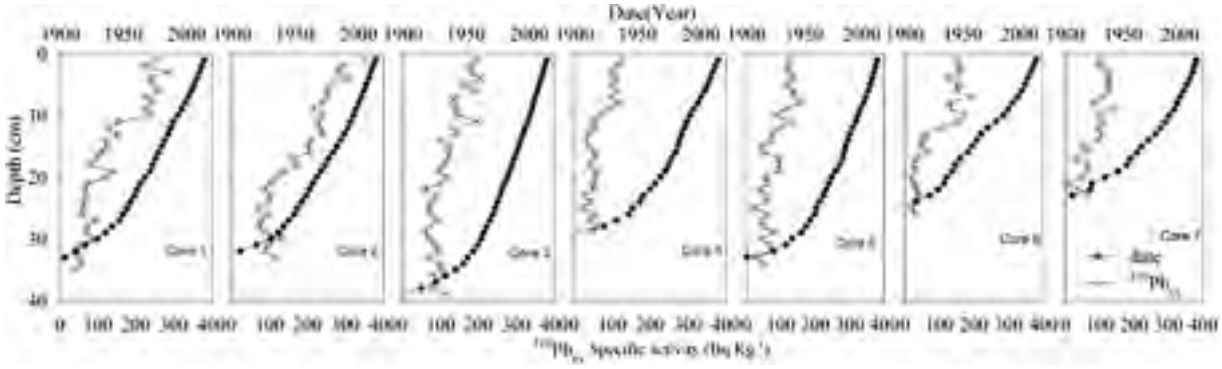

Fig. 2. Vertical distribution of $^{210}Pb_{ex}$ for each core. The geochronology of the sediment cores was estimated from the $^{210}Pb_{ex}$ CRS model and ^{137}Cs.

$$0 \le p_i \le 1 \text{ and } \sum_{i=1}^{n} p_i = 1,$$

where $C\text{-}m_{n\text{-Alkanes}}$ is the model *n*-alkanes concentration in the sediment, P_i is the percentage of the ith *n*-alkane, and *n* is the alkane number. The optimal target equation is

$$\text{Min}\left[\left(\left(C_{n\text{-Alkanes}} - \sum_{i=1}^{n}(C\text{-}g_{n\text{-Alkanes}} \times p_i)\right)/C_{n\text{-Alkanes}}\right)^2\right]. \quad (6)$$

The *n*-alkane numbers were obtained from cluster analysis, and five clusters were finally determined. Among of them, *n*-alkanes with significant allochthonous and autochthonous characteristics were selected as $C\text{-}g_{n\text{-Alkanes}}$ (Eckmeier and Wiesenberg, 2009; Choi and Lee, 2013; Feakins et al., 2016). Cluster analysis and the calculation of P_i were processed in MATLAB 7.9.0 (R2009b, MathWorks, USA).

3. Results

3.1. Distribution of $^{210}Pb_{ex}$ and dating

The vertical distribution of specific activity $^{210}Pb_{ex}$ in the profile of all sediments (7 cores) ranged from 5.58 to 355.56 Bq kg^{-1}, with a mean value of 109.58 ± 66.09 Bq kg^{-1} (mean value ± standard deviation). The highest $^{210}Pb_{ex}$, with a mean value of 176.23 ± 81.13 Bq kg^{-1}, located in core 2, was affected by intensive agriculture and Dahe and Caihe rivers. The relatively low $^{210}Pb_{ex}$ (65.48 ± 31.29 Bq kg^{-1}) in core 4 was near a floriculture greenhouse in Dounan. The period covered by each sedimentary core was longer than 100 years (the geochronology from 1900 to 2014 is shown in Fig. 2).

The geochronology estimated from the $^{210}Pb_{ex}$ CRS model was compared to the time markers from ^{137}Cs (1986, 1975, 1963 and 1954). The mean differences of geochronology between the results from $^{210}Pb_{ex}$ and ^{137}Cs are 1.08 ± 2.85 years, 3.27 ± 2.14 years, 2.04 ± 2.00 years and −3.49 ± 2.69 years for 1986, 1975, 1963 and 1954, respectively. The difference between these geochronologies was not significant in 1986 and 1963, with a = 0.05 [F(1.86) < F crit (4.23)], but was slightly significant in 1954 and 1975, with a = 0.05 [F(8.56) > F crit (7.72)], from one-way analysis of variance. The highest and lowest uncertainties (difference between the geochronology estimated from $^{210}Pb_{ex}$ and ^{137}Cs) were found in 1954 of core 2 (−8 years) and 1986 of core 3 (0.2 year).

3.2. Content sediment characteristics of TOC and TON

The concentrations of TOC and TON decreased gradually with vertical depth. The contents of TOC and TON ranged from 8.67 ± 5.82 mg g^{-1} in 1900 to 59.29 ± 31.33 mg g^{-1} in 2012, and 0.44 ± 0.27 mg g^{-1} in 1900 to 4.03 ± 1.19 mg g^{-1} in 2012 over a 112-year period (Fig. 3). The mean values of TOC and TON from 1900 to 1910 were 8.08 ± 4.20 mg g^{-1} and 0.43 ± 0.23 mg g^{-1}, while the mean values of TOC and TON increased to 42.18 ± 22.89 mg g^{-1} and 3.43 ± 1.36 mg g^{-1} from 1990 to 2000. TOC and TON increased approximately 4.33 and 7.34 times over this period, according to the analysis method proposed by Heathcote et al. (2015). Significant increases in TOC and TON were observed after 1970. The mean values of TOC and TON were 9.00 ± 4.64 mg g^{-1} and 0.62 ± 0.14 mg g^{-1} before 1970, and 37.62 ± 20.56 mg g^{-1} and 2.73 ± 0.90 mg g^{-1} after 1970. High TOC content was mainly located in southern and northern Dianchi. The highest TOC of 87.73 ± 9.66 mg g^{-1} (mean value between 1990 and 2012) was in core 6, and the lowest TOC was in the middle of the lake (Fig. 3A, core 3). The highest TON content was found in southern Dianchi, with a TON of 5.36 ± 0.52 mg g^{-1} (mean value between 1990 and 2012) in core 1 (Fig. 3 B).

The OCAR and ONAR in Dianchi rose over the years and ranged from 10.46 ± 1.95 g m^{-2} yr^{-1} in 1900 to 112 ± 50.62 g m^{-2} yr^{-1} in 2012 and 0.59 ± 0.31 g m^{-2} yr^{-1} in 1900 to 8.50 ± 2.51 g m^{-2} yr^{-1} in 2012, respectively. The OCAR and ONAR showed almost no change before the 1970s, with mean values of 15.09 ± 2.70 g m^{-2} yr^{-1} and 1.02 ± 0.35 g m^{-2} yr^{-1}, but they dramatically increased after the

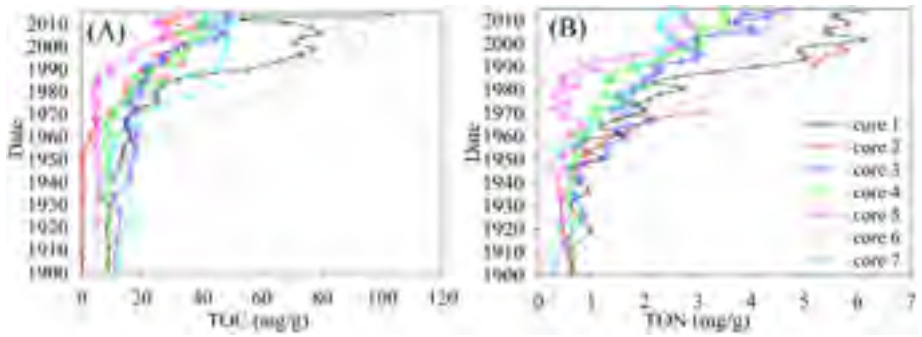

Fig. 3. Sediment profiles of total organic carbon and nitrogen. The geochronometry, dated from Pb^{210}, ranges from 1900 to 2012. Data before 1900 is not shown in the figure.

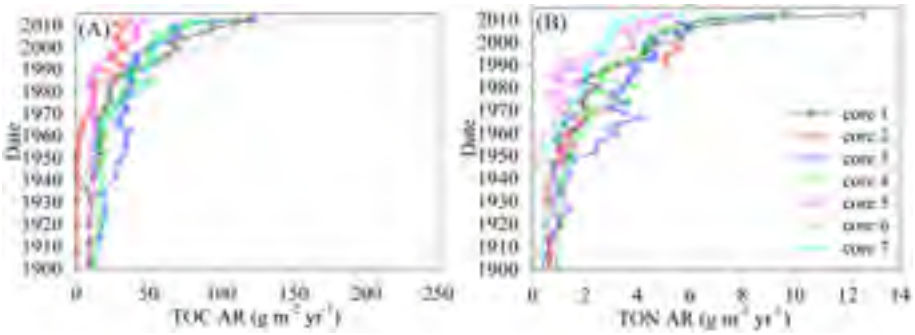

Fig. 4. Sediment profiles of total organic carbon and nitrogen accumulation rates from lake sediment cores in Dianchi.

1970s, with mean values of 48.52 ± 21.20 g m^{-2} yr^{-1} and 3.49 ± 1.50 g m^{-2} yr^{-1}, respectively. The OCAR and ONAR reached the highest values in surface sediment (Fig. 4). The OCAR and ONAR in core 3 increased starting in the 1950s, which is much earlier than other cores. The burial stock of OC during the past 28 years (1986–2014) (OC, 0.467 ± 0.0055 Tg and ON, 0.033 ± 0.0004 Tg) is almost equal to the storage of OC and ON from 1900 to 1985 (TOC, 0.468 ± 0.0022 Tg; ON, 0.032 ± 0.0002 Tg).

3.3. Occurrence and distributions of n-alkanes

The total concentrations of *n*-alkanes ($\sum$(*n*-C_{10} to *n*-C_{34})) ranged from 4145.9 to 67,547.6 ng g^{-1}, with a mean value of 16,838.4 ± 11,145.1 ng g^{-1}, in the sediment. The aliphatic hydrocarbon fractions were mainly composed of allochthonous-derived long-chain *n*-C_{27} to *n*-C_{31} alkanes and autochthonous-derived short-chain *n*-C_{17} alkanes (Fig. 5). Middle-chain *n*-C_{23} and *n*-C_{25} alkanes, derived from submerged and floating aquatic plants, were also observed in the sediment (cores 1, 5, 6 and 7 in Fig. 5) (Gao et al., 2015a, 2015b; Liu and Liu, 2016). The odd numbered n-alkanes in short-chain *n*-C_{17} alkane-dominated sediments (cores 2, 5, 6 and 7 in Fig. 5) are remarkable, indicating that the buried OC largely consisted of algae in these cores. High molecular-weight compounds with a significant preference for odd-numbered n-alkanes (*n*-C_{27} to *n*-C_{31}) were predominant in all sediment, reflecting that the terrestrial OC contributed significantly to sediment organic carbon burial. High molecular-weight compounds with even/odd numbered n-alkanes also could be found in the sediment (cores 3 and 6 in Fig. 5), which may have been caused by slash-and-burn cultivation from the 1920s to the 1930s (core 3 in Fig. 5) and modern fossil fuel combustion (2000s of core 6 in Fig. 5).

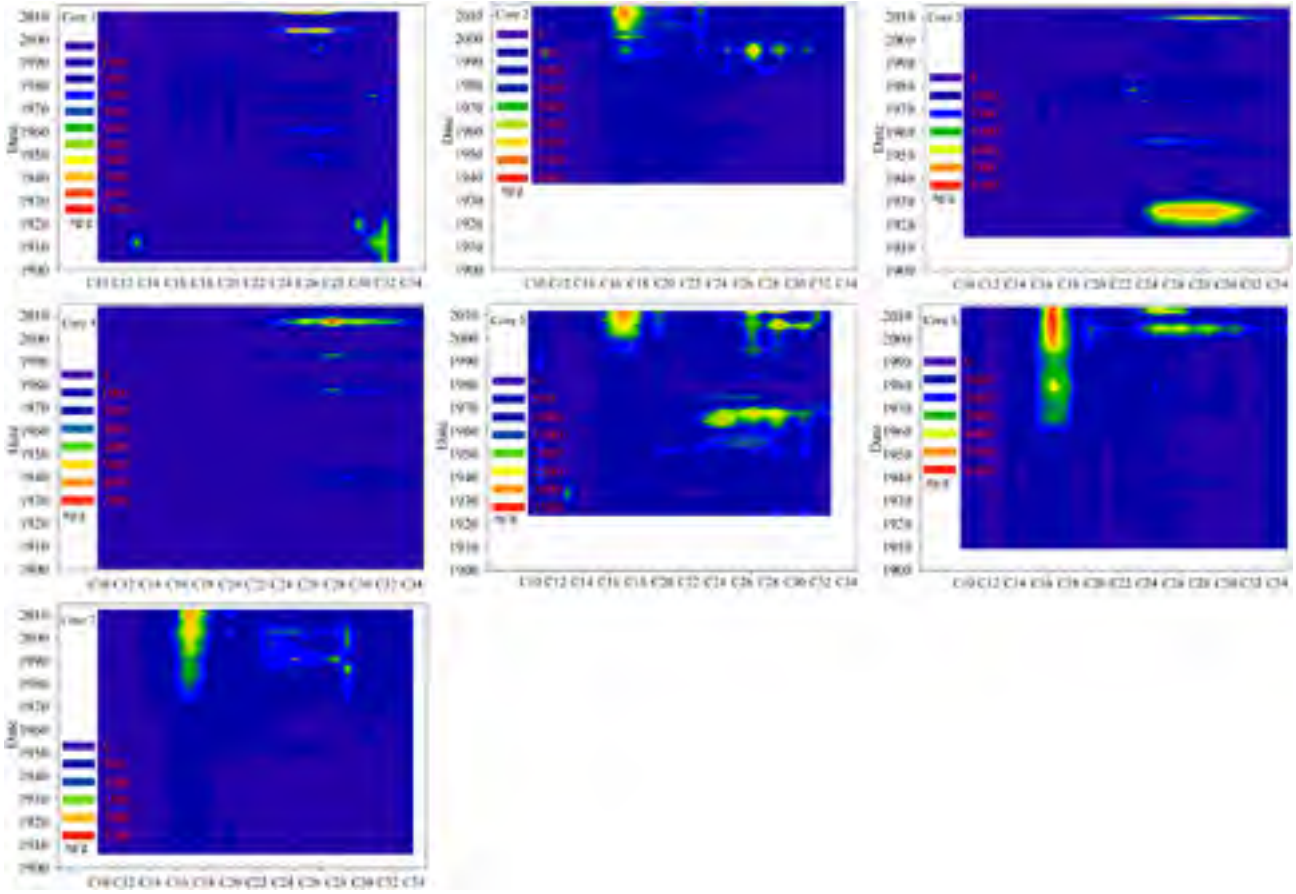

Fig. 5. Sediment profiles of *n*-alkanes for each sediment core. The allochthonous-derived long-chain *n*-alkanes and autochthonous-derived short-chain *n*-alkanes in the sediment are clearly shown.

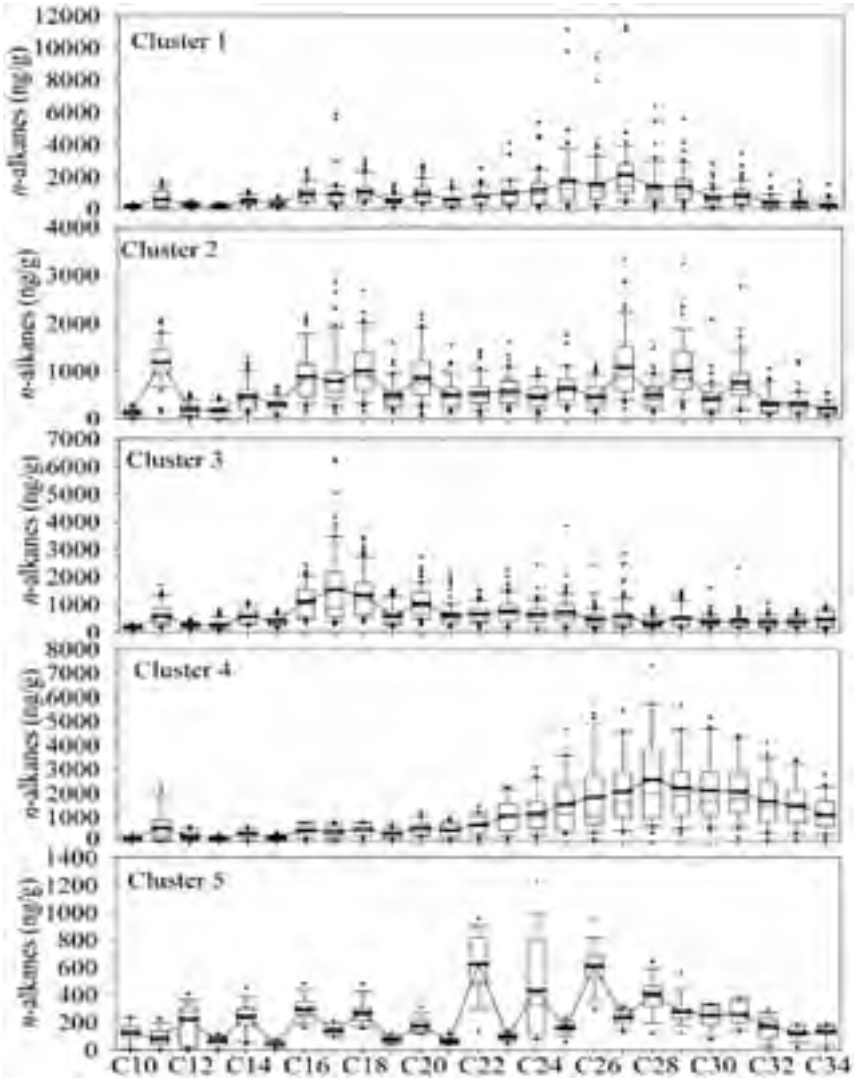

Fig. 6. Box drawing of *n*-alkane distributions for each category from cluster analysis. The boundary of the box indicates the 25th and 75th percentile of n-alkane, the gray line in the box is the median n-alkane value, and the black line is the mean n-alkane value. Five categories were identified by cluster analysis from seven cores of 213 samples.

3.4. Group characteristics of n-alkanes

Cluster analysis of the lipid biomarker data indicated five categories that meet the Akaike information criterion (Fig. 6). The *n*-alkanes of clusters 1 and 2 showed bimodal distributions, maximizing at *n*-C_{17} and *n*-C_{25} to *n*-C_{31}, indicating that both allochthonous and autochthonous sources have a significant effect on OC and ON burial (Cranwell et al., 1987; Zhao et al., 2003; Gao et al., 2015a, 2015b; Liu and Liu, 2016). The *n*-alkanes of cluster 3, with a unimodal distribution maximizing at *n*-$C_{17,}$ suggest autochthonous effects on OC and ON burial (Giger et al., 1980; Meyers, 2003). The unimodal distribution of *n*-alkanes in cluster 4, with a mean odd-even preference (OEP) value of 1.13 ± 0.21, indicated an allochthonous source of OC and ON burial (Pearson and Eglinton, 2000; Ortiz et al., 2011; Silva et al., 2012). The *n*-alkanes in cluster 5, with a significantly even carbon number preference (OEP = 0.21 ± 0.08) manifested from the degradation of bacteria and fossil fuel combustion (Han and Calvin, 1969; Lü and Zhai, 2006; Fang et al., 2014). Pristane (Pr) and phytane (pH), expressed as a ratio (Pr/Ph) representing anoxic conditions (Didyk et al., 1978), were detected in all samples. Most Pr/Ph values (core 1: 0.85 ± 0.10; core 2: 0.36 ± 0.12; core 3: 0.36 ± 0.20; core 4: 0.34 ± 0.21; core 5: 0.76 ± 0.19; core 6: 0.63 ± 0.24; core 7: 0.35 ± 0.16) were smaller than 1, indicating anoxic conditions in the sediment of Dianchi. This may be the reason for the obvious even carbon number preference in the sediment.

Clusters 1, 2 and 4 presented much higher concentrations of TOC and TON than clusters 3 and 5 (Table 1). The OCAR and ONAR in each cluster showed similar trends to TOC and TON, indicating that terrestrial particulates contained much more TOC and TON than planktonic particulates. The ratio of TOC to TON (TOC/TON), which is a useful indicator for identifying the organic sources of sediments, showed a relatively low value in cluster 3 and a high value in cluster 4. This is consistent with the cluster analysis results, showing that clusters 3 and 4 refer to contributions of autochthonous and allochthonous sources, respectively. The proxies of *n*-alkanes for each cluster are shown in Table 1. The carbon preference index (CPI), calculated from *n*-alkane distributions, was between 0 and 4 in most samples, suggesting that *n*-alkanes had a mixed origin. The natural *n*-alkane ratio (NAR) indicates that the terrestrial source of *n*-alkanes was of mixed origin, such as petroleum hydrocarbons and higher plants (Wang et al., 2008). The relatively low OEP suggests that the source of the *n*-alkanes mixed with petroleum and was also accompanied by strong bacterial activities or low terrestrial plant debris flux (Meyers and Ishiwatari, 1993). The ratio of short-chain (C_{15}–C_{20}) to high-chain (C_{21}–C_{34}) *n*-alkanes (LMW/HMW) suggests that cluster 3

Table 1
Mean value of proxies of n-alkanes and organic carbon and nitrogen for each cluster (TOC and TON, mg g^{-1}; OCAR and ONAR, g m^{-2} yr^{-1}), 27.16 ± 22.62 indicates the mean value ± standard error.

Clusters	Cluster 1	Cluster 2	Cluster 3	Cluster 4	Cluster 5
TOC	27.16 ± 22.62	24.03 ± 19.70	18.62 ± 22.88	27.59 ± 18.17	15.38 ± 12.22
TON	2.28 ± 1.56	2.27 ± 1.77	1.61 ± 1.19	2.18 ± 1.49	1.40 ± 0.97
TOC/TON	12.13 ± 4.94	11.33 ± 2.77	10.45 ± 6.08	14.06 ± 4.18	10.85 ± 2.16
TOC/TOP	49.59 ± 43.19	38.74 ± 33.83	69.10 ± 70.15	50.37 ± 28.79	32.55 ± 25.63
OCAR	38.66 ± 34.01	33.21 ± 26.79	26.85 ± 24.07	45.40 ± 27.56	30.55 ± 27.22
ONAR	3.28 ± 2.28	3.08 ± 2.22	1.72 ± 1.41	3.74 ± 2.48	2.81 ± 2.27
CPI1	1.05 ± 0.20	1.18 ± 0.33	0.94 ± 0.18	0.93 ± 0.17	0.45 ± 0.09
CPI2	1.88 ± 0.62	2.26 ± 0.60	1.33 ± 0.63	1.10 ± 0.26	1.03 ± 0.38
NAR	0.11 ± 0.10	0.20 ± 0.14	0.07 ± 0.08	0.03 ± 0.11	−0.34 ± 0.11
OEP	1.08 ± 0.29	1.28 ± 0.53	1.16 ± 0.37	1.13 ± 0.21	0.21 ± 0.08
LMW/HMW	0.37 ± 0.12	0.57 ± 0.17	0.82 ± 0.21	0.14 ± 0.07	0.27 ± 0.09
Paq	0.51 ± 0.14	0.43 ± 0.82	0.60 ± 0.11	0.37 ± 0.05	0.33 ± 0.06
ACL	27.27 ± 0.56	27.67 ± 0.49	27.35 ± 0.55	28.39 ± 0.30	27.61 ± 0.50
C31/C19	1.96 ± 1.22	1.57 ± 0.54	0.80 ± 0.44	7.35 ± 4.10	3.80 ± 1.94

CPI1 = ∑odd(C15-C34)/∑even(C15-C34), CPI2 = (C27 + C29 + C31 + C33) (C28 + C30 + C32 + C34), NAR = [∑(C28-C30)-2∑even(C20 + C32)]/∑(C19-C33), LMW/HMW = ∑(C15–C20)/∑(C21–C34), ACL = [(25(C25) + 27(C27) + 29(C29) + 31(C31) + 33(C33)]/(C25 + C27 + C29 + C31 + C33), Paq = (C23 + C 25)/(C23 + C25 + C29 + C31), OPE = (C25 + 6C27+ C29)/(4C26 + 4C28) (Sojinu et al., 2010; Ortiz et al., 2016).

(LMW/HMW close to 1) represents planktonic sources and cluster 4 represents terrestrial sources (LMW/HMW close to 0) (Commendatore et al., 2000; Stout et al., 2002; Wang and Fingas, 2005). The relatively high Paq proxy in cluster 3 indicates that autochthonous-source *n*-alkanes were highly contributed to by aquatic macrophytes (Ficken et al., 2000; Hockun et al., 2016). The low variation in the average chain length (ACL) was due to the low input of petrogenic hydrocarbons (Jeng, 2006). The *n*-alkane ratio (C31/C19), characterized by the relative proportions of allochthonous and autochthonous inputs, suggests that clusters 3 and 4 represent planktonic and terrestrial sources, respectively (Simoneit et al., 1990).

Cluster analysis filtered out three types of *n*-alkanes, with allochthonous (cluster 4), autochthonous (cluster 3) and mixed origin (cluster 1, 2 and 5) characteristics. The *n*-alkanes in Clusters 3 and 4 with significant allochthonous and autochthonous characteristics were treated as the end members of the multi-source mixing model ($C\text{-}g_{n\text{-Alkanes}}$ in Eq. (5)).

3.5. Source of TOC identified from n-alkanes

The contributions of algae and direct human activities to OC, estimated by a multi-source mixing model, showed that both algae and direct human activities contributed to the increased OCAR and ONAR (Fig. 7). ON was coupled with OC for each sedimentary core and was not described separately. Direct human activities observably increased OCAR and showed an especially controlled effect in cores 1, 3 and 4 (Fig. 8, line with solid circle), which are distributed in eastern Dianchi (which is close to large areas of farmland). The time the OCAR increase began for core 4 (1970s) is much earlier than cores 1 (1980s) and 3 (1990s) due to the intensity of nearby human activities (Huang et al., 2014). The contribution of direct human activities accounted for 85.14 ± 9.96% (core 1), 93.88 ± 9.70% (core 3) and 98.18 ± 3.79% (core 4) of the OCAR increase since the 1970s. This is consistent with previous studies, showing that land-use cover change (LUCC) and intensive agriculture controlled the burial rate of organic carbon (Heathcote and Downing, 2012; Anderson et al., 2013). Algae, treated as an autochthonous source of organic carbon, also significantly increased OCAR, as in cores 2, 5, 6 and 7 (Fig. 8, line with hollow circle). The increase in OCAR parallels the rise of autochthonous sources (algae) since the 1990s (Fig. 8). Algae and direct human activities became dominant during the 1970s (core 7 in Fig. 7), 1980s (core 2 in Fig. 8) and 2000s (core 5 in Fig. 7). This is in accordance with the occurrences of eutrophication and algal blooms in Dianchi (Huang et al., 2014). The contribution of algae to the increased OCAR changed from 20.86 to 97.82% (73.04 ± 21.36%, core 2), from 17.98 to 94.29% (40.92 ± 25.48%, core 5), from 63.36 to 97.01% (87.04 ± 14.22%, core 6) and from 23.07 to 86.70% (64.31 ± 11.51%, core 7) since the 1970s. This confirms that eutrophication and algal blooms enhanced OC burial in eutrophic lakes, as proposed by previous studies (Downing et al., 2008; Heathcote and Downing, 2012; Anderson et al., 2014; Wu et al., 2016). Direct human activity was the primary contributor to the increasing OCAR in eastern lake sediment (cores 1, 3, 4) while algae was the primary contributor in northern and western lake sediment (cores 2, 5, 6, 7). This is further corroborated by the distribution of LUCC and algal blooms. Intense LUCC mainly occurred around the eastern part of the lake, and algal blooms primarily spread over the northern and western areas of the lake (Figs. 6 and 7 in Huang et al., 2014). The contribution of direct human activities and algae to OCAR, which was determined from n-alkanes, improves our quantitative understanding of the reasons for increases in OCAR and ONAR.

4. Discussion

4.1. Validation of the multi-source mixing model

The multi-source mixing model (Eqs. (5) and (6)) was applied to identify the allochthonous and autochthonous origins of the sedimentary cores. The *n*-alkanes with significant allochthonous and autochthonous characteristics in Clusters 3 and 4 were treated as the end members of the multi-source mixing model. However, the end members from clusters 3 and 4 were not characterized only by

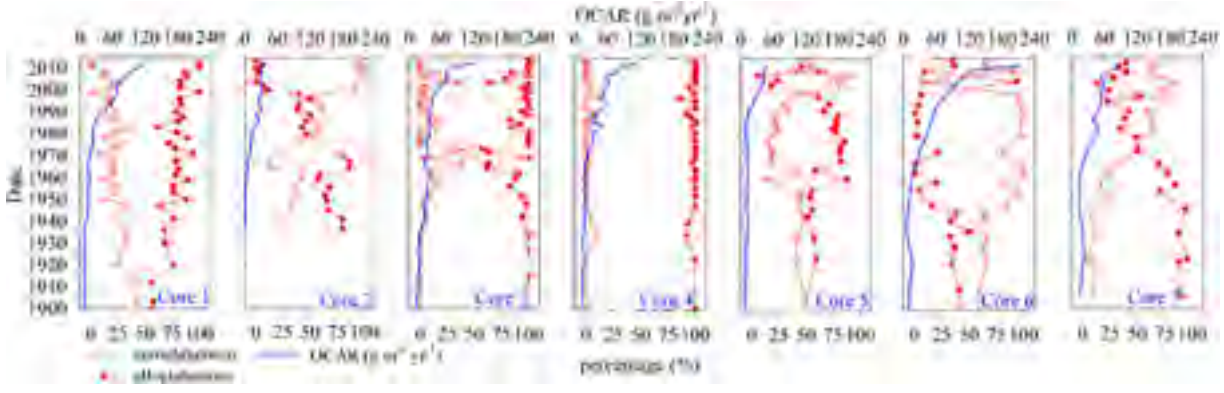

Fig. 7. Contributions of allochthonous and autochthonous sources of organic carbon to organic carbon accumulation rates for each sedimentary core.

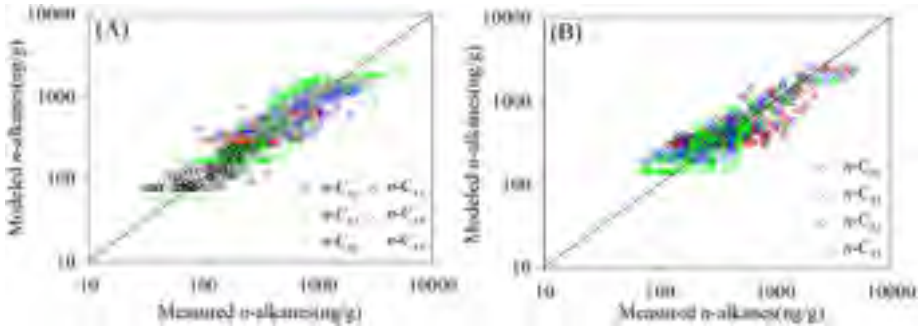

Fig. 8. Comparison of measured and modeled n-alkanes for short- (A) and long-chain n-alkanes (B). The consistency between measured and modeled n-alkanes indicates the validated result from the multi-source mixing model.

autochthonous and allochthonous origins, respectively. For example, some algae (such as diatoms and Hippuris) can generate long-chain *n*-alkanes (Sinninghe Damsté et al., 1999; Aichner et al., 2010). Meanwhile, *n*-alkanes contaminated by petroleum and strong bacterial activities can also disturb the estimation of allochthonous and autochthonous origin. The correlation coefficients between measured and modeled *n*-alkanes are >0.75, with mean values of 0.84 (n-C_{13}–n-C_{18}) and 0.81 (n-C_{30}–n-C_{33}). A comparison of measured and modeled *n*-alkanes (Fig. 8) indicates that the estimated percentages of allochthonous and autochthonous (P_i in Eq. (5)) sources is valid for modelling *n*-alkanes in each depth of the sediment cores. Consequently, this multi-source mixing model is flexible and can estimate the relative contributions of algae (autochthonous) and human activities (allochthonous) to the increases in OC and ON.

4.2. Influencing factors on the variation of allochthonous and autochthonous sources

4.2.1. Eutrophication and algal blooms

It has been confirmed, in this and previous studies, that both human activities and algae biomass increase OCAR and ONAR (e.g., Heathcote and Downing, 2012; Anderson et al., 2013, 2014). It is also important to understand the detailed relationship between human activities and trophic proxies to OCAR and ONAR, although these relationships vary among lakes. The concentration of total nitrogen (TN_w) in the water of Dianchi Lake is highly correlated to the concentration of chlorophyll-a (Chl-a) (Chl-a = 139.28*TN_w-120.4, $R^2 = 0.85$, $N = 77$, $p < 0.0001$, scatter diagram not shown in this study) and can be treated as the proxy of phytoplankton biomass in Dianchi Lake. The high correlation of TN_w to OCAR ($R^2 = 0.71$, $p < 0.0001$) and ONAR ($R^2 = 0.66$, $p < 0.001$) strongly suggests that algae increased OCAR and ONAR in Dianchi Lake (Fig. 9A). The strong effects of terrestrial input on OCAR and ONAR present a linear function of TN_w, with growth rates of approximately 33.44 and 2.392, respectively. The high value (33.44) is much higher than the growth rate of OCAR due to chlorophyll-a in a study by Anderson et al. (2013). The concentration of total phosphorus in the water has almost no correlation to OCAR and ONAR due to the extreme abundance of phosphorus in Dianchi Basin (Fig. 9B).

4.2.2. Human activities

Developed land area and fertilization intensity represent the most intense human activities. To examine the correlation between human activities and OC and ON burial, we compared OCAR and ONAR with the historical land use of developed land (as an indicator of human activities), as well as nitrogenous fertilization (Buffam et al., 2011; Heathcote and Downing, 2012). The area of developed land (A_{CL}) increased by a factor of 11.62 from 1974 to 2012 and showed a significant correlation between OCAR ($R^2 = 0.86$, $N = 38$, $p < 0.0001$), ONAR ($R^2 = 0.83$, $N = 38$, $p < 0.0001$) and increases in developed land (Fig. 10A) due to the destruction of the earth's surface during construction. Large amounts of topsoil were lost with the transformation of farm land to developed land (Alström and Bergman, 1988; Quinton et al., 2010). OCAR and ONAR increased by 0.0694 g m^{-1} yr^{-1} and 0.0047 g m^{-1} yr^{-1}, respectively, with an increase of 1 km^2 A_{CL}, suggesting that increases in OCAR and ONAR are associated with landscape changes from the intensification of human activities (Heathcote and Downing, 2012). High-intensity agricultural cultivation not only increased the nutrients in the lake water but also promoted OC and ON burial in the sediment (Heathcote and Downing, 2012; Anderson et al., 2013). A high correlation between nitrogenous fertilizer and OCAR ($R^2 = 0.93$, $N = 31$, $p < 0.0001$) and ONAR ($R^2 = 0.96$, $N = 31$, $p < 0.0001$) supports results from previous studies (Fig. 10B) (Heathcote and Downing, 2012; Anderson et al., 2013). OCAR and ONAR increased by 8.23 g m^{-1} yr^{-1} and 0.56 g m^{-1} yr^{-1} per 1 t km^{-2} yr^{-1} nitrogenous fertilization. Thus, high-intensity human activities (urbanization and agricultural cultivation) significantly accelerate OC and ON burial.

4.2.3. Elasticity of driving factors

The effects of other influencing factors (such as climatic change, economic development, population growth, etc.) on OCAR and ONAR are

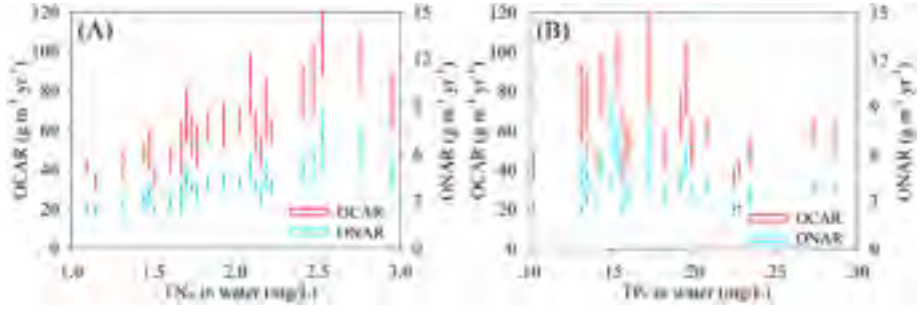

Fig. 9. Relationships between nutrients (TN and TP) in the water of Dianchi and OCAR and ONAR. The relationship between TN and OCAR is OCAR = 33.44* TNw-4.06 (R2 = 0.66, N = 26, p < 0.001) and the relationship between TN and ONAR is ONAR = 2.392* TNw-0.306 (R2 = 0.71, N = 26, p < 0.0001), from 1987 to 2012.

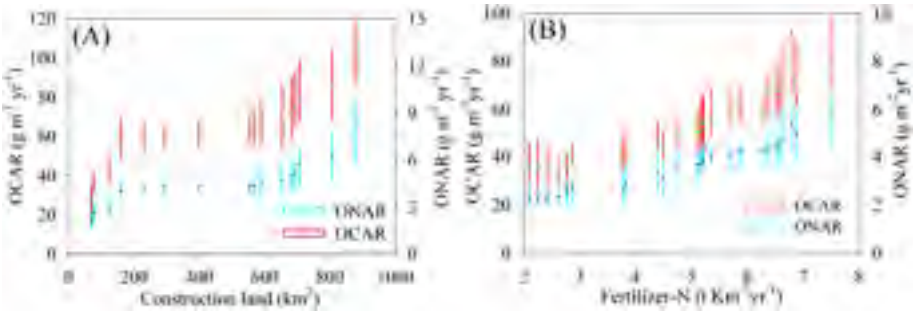

Fig. 10. A) Relationships between developed land area (A_{CL}) and OCAR and ONAR. The relationship between A_{CL} and OCAR was OCAR = 0.0694* A_{CL} + 33.096 (R^2 = 0.86, N = 39, p < 0.0001), and the relationship between A_{CL} and ONAR was ONAR = 0.0047* A_{CL} + 2.4333 (R^2 = 0.83, N = 39, p < 0.0001), from 1974 to 2012. B) Relationships between fertilizer (NF) and OCAR and ONAR. The relationship between NF and OCAR was OCAR = 8.223* NF + 14.617 (R^2 = 0.93, N = 31, p < 0.0001), and the relationship between NF and ONAR was ONAR = 0.560* NF + 1.144 (R^2 = 0.91, N = 31, p < 0.0001), from 1980 to 2010.

much more complex than the relationships shown in Figs. 8 and 9 (Quinton et al., 2010; Kortelainen et al., 2013; Anderson et al., 2013, 2014; Ferland et al., 2014; Fortino et al., 2016). There also exist complex linkages among these influencing factors. The STIRPAT model (York et al., 2003), which has been widely applied in the analyses of carbon dioxide emissions and environmental change (Zhou et al., 2015; Zhou and Liu, 2016), was used to estimate the elasticity of OCAR and ONAR for each influencing factor (Fig. 11). It was obvious that population (PO) growth, economic development (FI, SI and TI), LUCC (FO, FA, CL and BL) and climatic change (temperature, TE) significantly affected OCAR and ONAR. Population was the primary influencing factor; a 1% increase in population resulted in 37.53% and 28.76% increases in OCAR and ONAR, respectively. Economic development caused 28.34% and 19.20% increases in OCAR and ONAR, respectively, with a 1% increase in secondary industry. LUCC is also a very important factor controlling OCAR and ONAR. Forest land (FO) reduced OCAR and ONAR by 13.60% and 29.51%, respectively, with a 1% increase in FO area. Conversely, farm (FA) and construction land (CL) increased OCAR (and ONAR) by 11.56% (and 9.87%) and 10.00% (and 1.98%) with a 1% increase in FA and CL area. A 1% increase in fertilization stimulates OCAR and ONAR by 6.27% and 0.71%, respectively, and the nutrients in lake water and total nitrogen in the water (TN_w) will lead to 2.88% and 11.30% increases in OCAR and ONAR.

Climate change, such as temperature change, is also tied to OCAR (Brothers et al., 2008; Kosten et al., 2010). Temperature (TE) induced 26.09% and 24.01% increases in OCAR and ONAR, respectively, with a 1% increase in TE. The temperature in Dianchi Basin increased from 14.3 °C to 17.3 °C from 1974 to 2012 and is positively correlated to OCAR (OCAR = 20.247*T-261.09, R^2 = 0.69, N = 43) and ONAR (ONAR = 1.4122*T-18.099, R^2 = 0.68, N = 43), especially after the 1980s, when algal blooms began to occur frequently in Dianchi Lake. This may indicate that temperature promoted the growth of algae, which is supported by in-situ observation data (Zhou et al., 2016).

5. Conclusions

The historical records of TOC and TON content in the sediment of Dianchi indicated that TOC and TON rose by factors of approximately 9.1 and 6.8, respectively, from 1900 to 2012. TOC and TON dramatically increased after the 1970s. Meanwhile, OCAR and ONAR rose by factors of 4.33 and 7.34 over the past hundred years and showed a significant increase after the 1970s. The allochthonous-derived long-chain n-C_{27} to n-C_{31} alkanes and autochthonous-derived short-chain n-C_{17} alkanes observed in the sediment suggest that both allochthonous and autochthonous sources controlled OCAR and ONAR, but the ratio of allochthonous to autochthonous sources exhibited significant spatial and temporal variation. The prominent contribution of allochthonous sources (human activities) to the increase in OCAR was mainly located in eastern and southern Dianchi Lake. The dominant contribution of autochthonous sources (algae) to the increase of OCAR was mainly distributed in northern and western Dianchi Lake.

Globally intensified eutrophication will fix more CO_2 in inland water and enhance the burial stock of OC and ON in inland water sediment. As C is lost in the surface soil with accelerated human activities, increases of OCAR and ONAR in inland water sediment and CO_2 in the atmosphere will strongly regulate the global carbon cycle. However, human activity is a complex process (such as LUCC, economic development, population growth, etc.). The effects of human activities on eutrophication, OCAR

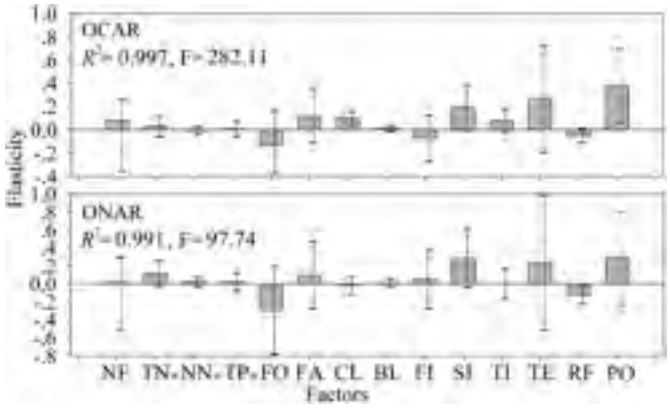

Fig. 11. Elasticities of OCAR and ONAR for each influencing factor. Bars are the estimated elasticity, while error bars are the 95% confidence interval values for each influencing factor. Elasticity indicates that a 1% variation of the independent variables (influencing factors) caused percentage changes of the dependent variables (OCAR and ONAR). NF: nitrogenous fertilizer, TN_w: total nitrogen in the water, NN_w: ammonia nitrogen in the water, TP_w: total phosphorus in the water, FO: forest land, FA: farm land, CL: construction land, BL: bare land, FI: primary industry, SI: secondary industry, TI: tertiary industry, TE: temperature, RF: rainfall, PO: population.

and ONAR are indistinct, and the role of eutrophication in the global carbon cycle is still unclear. Thus, more studies are required to understand the processes of carbonic transmission and transformation, especially for inland waters.

Acknowledgments

This study was supported by the National Natural Science Foundation of China (Grant Nos. 41503075, 41673108 and 41571324) and funded by the Priority Academic Program Development of Jiangsu Higher Education Institutions, the State Key Laboratory of Lake Science and Environment (2016SKL005) and the China Postdoctoral Science Foundation Funded Project (2015M581826). Support from A-Xing Zhu through the Vilas Associate Award, the Hammel Faculty Fellow Award, the Manasse Chair Professorship from the University of Wisconsin-Madison, and the "One-Thousand Talents" Program of China is greatly appreciated. We are grateful to Nick Kleeman for the language editing. We are also grateful to Professor Zucong Cai for his valuable suggestions and the useful comments from three anonymous reviewers.

References

Aichner, B., Wilkes, H., Herzschuh, U., Mischke, S., Zhang, C.J., 2010. Biomarker and compound specific $\delta^{13}C$ evidence for changing environmental conditions and carbon limitation at Lake Koucha, eastern Tibetan Plateau. J. Paleolimnol. 43, 873–899.

Alin, S.R., Johnson, T.C., 2007. Carbon cycling in large lakes of the world: a synthesis of production burial, and lake-atmosphere exchange estimates. Glob. Biogeochem. Cycles 21, 126.

Alström, K., Bergman, A., 1988. Sediment and nutrient losses by water erosion from arable land in south Sweden: a problem with nonpoint pollution. Vatten 44, 193–204.

Anderson, N.J., Bennion, H., Lotter, A.F., 2014. Lake eutrophication and its implications for organic carbon sequestration in Europe. Glob. Chang. Biol. 20, 2741–2751.

Anderson, N.J., Dietz, R.D., Engstrom, D.R., 2013. Land-use change, not climate, controls organic carbon burial in lakes. B Biol. Sci]–>Proc. R. Soc. B Biol. Sci. 280, 3907–3910.

Appleby, P.G., 2008. Three decades of dating recent sediments by fallout radionuclides: a review. The Holocene 18, 83–93.

Bastviken, D., Tranvik, L.J., Downing, J.A., Crill, P.M., Prast, E.A., 2011. Freshwater methane emissions off set the continental carbon sink. Science 331, 50.

Buffam, I., Turner, M.G., Desai, A.R., Hanson, P.C., Rusak, J.A., Lottig, N.R., Stanley, E.H., Carpenter, S.R., 2011. Integrating aquatic and terrestrial components to construct a complete carbon budget for a north temperate lake district. Glob. Chang. Biol. 17, 1193–1211.

Brothers, S., Vermaire, J.C., Gregory-Eaves, I., 2008. Empirical models for describing recent sedimentation rates in lakes distributed across broad spatial scales. J. Paleolimnol. http://dx.doi.org/10.1007/s10933-008-9212-8.

Cardoso, S.J., Enrich-Prast, A., Pace, M.L., Roland, F., 2014. Do models of organic carbon mineralization extrapolate to warmer tropical sediments. Limnol. Oceanogr. 59 (1), 48–54.

Chen, F.X., Fang, N.F., Wang, Y.X., Tong, L.S., Shi, Z.H., 2017. Biomarkers in sedimentary sequences: indicators to track sediment sources over decadal timescales. Geomorphology 278, 1–11.

Chmiel, H.E., Niggeman, J., Koki, J., Ferland, M.E., Dittmar, T., Sobek, S., 2015. Uncoupled organic matter burial and quality in boreal lake sediments over the Holocene. J. Geophys. Res. Biogeosci. 120, 1751–1763.

Choi, Y.J., Lee, S.Y., 2013. Microbial production of short-chain alkanes. Nature 502, 571–574.

Cole, J.J., Prairie, Y.T., Caraco, N.F., McDowell, W.H., Tranvik, L.J., Striegl, R.G., Duarte, C.M., Kortelainen, P., Downing, J.A., Middelburg, J.J., Melack, J.M., 2007. Plumbing the global carbon cycle: integrating inland waters into the terrestrial carbon budget. Ecosystems 10, 171–184.

Commendatore, M.G., Esteves, J.L., Colombo, J.C., 2000. Hydrocarbons in coastal sediments of Pat-agonia, Argentina: levels and probable sources. Mar. Pollut. Bull. 40, 989–998.

Cranwell, P.A., Eglinton, G., Robinson, N., 1987. Lipids of aquatic organisms as potential contributors to lacustrine sediments-II. Org. Geochem. 11, 513–527.

Damsté, J.S.S., Rijpstra, W.I.C., Schouten, S., Peletier, H., Maarel, M.J.E.C.V., Gieskes, W.W.C., 1999. A C_{25} highly branched isoprenoid alkene and C_{25} and C_{27}n-polyenes in the marine diatom *Rhizosolenia setigera*. Org. Geochem. 30, 95–100.

Didyk, B.M., Simoneit, B.R.T., Brassell, S.C., Eglinton, G., 1978. Organic geochemical indicators of paleo environmental conditions of sedimentation. Nature 272, 216–222.

Dietz, T., Rosa, E.A., 1994. Rethinking the environmental impacts of population, affluence and technology. Hum. Ecol. Rev. 1, 277–300.

Dong, X., Anderson, N.J., Yang, X., Chen, X., Shen, J., 2012. Carbon burial by shallow lakes on the Yangtze floodplain and its relevance to regional carbon sequestration. Glob. Chang. Biol. 18, 2205–2217.

Downing, J.A., Cole, J.J., Middelburg, J.J., Striegl, R.G., Duarte, C.M., Kortelainen, P., Prairie, Y.T., Laube, K.A., 2008. Sediment organic carbon burial in agriculturally eutrophic impoundments over the last century. Glob. Biogeochem. Cycles 22, 57.

Eckmeier, E., Wiesenberg, G.L.B., 2009. Short-chain n-alkanes (C 16–20) in ancient soil are useful molecular markers for prehistoric biomass burning. J. Archaeol. Sci. 36, 1590–1596.

Fang, J.D., Wu, F.C., Xiong, Y.Q., Li, F.S., Du, X.M., An, D., Wang, L.F., 2014. Source characterization of sedimentary organic matter using molecular and stable carbon isotopic composition of n-alkanes and fatty acids in sediment core from Lake Dianchi, China. Sci. Total Environ. 473–474, 410–421.

Ferland, M.E., Prairie, Y.T., Teodoru, C., Giorgio, P.A., 2014. Linking organic carbon sedimentation, burial efficiency, and long-term accumulation in boreal lakes. J. Geophys. Res. Biogeosci. 119, 836–847.

Feakins, S.J., Peters, T., Wu, M.S., Shenkin, A., Salinas, N., Girardin, C.A.J., Bentley, L.P., Blonder, B., Enquist, B.J., Martin, R.E., Asner, G.P., Malhi, Y., 2016. Production of leaf wax n -alkanes across a tropical forest elevation transect. Org. Geochem. 100, 89–100.

Ficken, K.J., Li, B., Swain, D.L., Eglinton, G., 2000. An n-alkane proxy for the sedimentary input of submerged/floating freshwater aquatic macrophytes. Org. Geochem. 31, 745–749.

Fortino, K., Whalen, S.C., Smoak, J.M., 2016. Patterns in the percent sediment organic matter of arctic lakes. Hydrobiologia 777, 149–160.

Gälman, V., Rydberg, J., de-Luna, S.S., Bindler R., Renberg, I., 2008. Carbon and nitrogen loss rates during aging of lake sediment: changes over 27 years studied in varved lake sediment. Limnol. Oceanogr. 53, 1076–1082.

Gao, L., Guimond, J., Thomas, E., Huang, Y., 2015a. Major trends in leaf wax abundance, δ^2H and $\delta^{13}C$ values along leaf venation in five species of C_3 plants: physiological and geochemical implications. Org. Geochem. 78, 144–152.

Gao, L., Hou, J., Toney, J., MacDonald, D., Huang, Y., 2011. Mathematical modeling of the aquatic macrophyte inputs of mid-chain n-alkyl lipids to lake sediments: implications for interpreting compound specific hydrogen isotopic records. Geochim. Cosmochim. Acta 75, 3781–3791.

Gao, W., Howarth, R.W., Swaney, D.P., Hong, B.G., Guo, H.C., 2015b. Enhanced N input to Lake Dianchi Basin from 1980 to 2010: drivers and consequences. Sci. Total Environ. 505, 376–384.

Giger, W., Schaffner, C., Wakeham, S.G., 1980. Aliphatic and olefinic hydrocarbons in recent sediments of Greifensee, Switzerland. Geochim. Cosmochim. Acta 44, 119–129.

Gudasz, C., Bastviken, D., Premke, K., Steger, K., Tranvik, L.J., 2012. Constrained microbial processing of allochthonous organic carbon in boreal lake sediments. Limnol. Oceanogr. 57, 163–175.

Gudasz, C., Bastviken, D., Steger, K., Premke, K., Sobek, S., Tranvik, L.J., 2010. Temperature-controlled organic carbon mineralization in lake sediments. Nature 466, 478–481.

Han, J., Calvin, M., 1969. Hydrocarbon distribution of algae and bacteria and microbiological activity in sediments. PNAS 64, 103–126.

Heathcote, A.J., Anderson, N.J., Prairie, Y.T., Engstrom, D.R., Giorgio, P.A., 2015. Large increases in carbon burial in northern lakes during the Anthropocene. Nat. Commun. 26, 1–6.

Heathcote, A.J., Downing, J.A., 2012. Impacts of eutrophication on carbon burial in Freshwater Lakes in an intensively agricultural landscape. Ecosystems 15, 60–70.

He, J., Xu, X.M., Yang, Y., Wu, X., Wang, L., Li, S., Zhou, H.B., 2015. Problems and effects of comprehensive management of water environment in Lake Dianchi. J. Lake Sci. 27 (2):195–199. http://dx.doi.org/10.18307/2015.0201.

Hockun, K., Mollenhauer, G., Ho, S.L., Hefter, J., Ohlendorf, C., Zolitschka, B., Mayr, C., Lücke, A., Schefuß, E., 2016. Using distributions and stable isotopes of n-alkanes to disentangle organic matter contributions to sediments of Laguna Potrok Aike, Argentina. Org. Geochem. 102, 110–119.

Huang, C.C., Wang, X.L., Yang, H., Li, Y.M., Wang, Y.H., Chen, X., Xu, L.J., 2014. Satellite data regarding the eutrophication response to human activities in the plateau lake Dianchi in China from 1974 to 2009. Sci. Total Environ. 485–486, 1–11.

Isidorova, A., Bravo, A.G., Riise, G., Bouchet, S., Björn, E., Sobek, S., 2016. The effect of lake browning and respiration mode on the burial and fate of carbon and mercury in the sediment of two boreal lakes. J. Geophys. Res. Biogeosci. 121, 233–245.

Jeng, W.L., 2006. Higher plant n-alkane average chain length as an indicator of petrogenic hydrocarbon contamination in marine sediments. Mar. Chem. 102, 242–251.

Johnson, M.S., Lehmann, J., Riha, S.J., Krusche, A.V., Richey, J.E., Ometto, J.P.H.B., Couto, E.G., 2008. CO_2 efflux from Amazonian headwater streams represents a significant fate for deep soil respiration. Geophys. Res. Lett. 35, 254–268.

Kortelainen, P., Rantakari, M., Pajunen, H., Huttunen, J.T., Mattsson, T., Juutinen, S., Larmola, T., Alm, J., Silvola, J., Martikainen, P.J., 2013. Carbon evasion/accumulation ratio in boreal lakes is linked to nitrogen. Global Biogeochem. Cycles 27, 363–374.

Kastowski, M., Hinderer, M., Vecsei, A., 2011. Long-term carbon burial in European lakes: analysis and estimate. Glob. Biogeochem. Cycles 25, 369–380.

Kosten, S., Roland, Marques, F. D. M. L. D. M., Van Nes, Mazzeo, E.H., Sternberg, N., Scheffer, L.L. da S.L., Cole, M., J., J., 2010. Climate-dependent CO_2 emissions from lakes. Glob. Biogeochem. Cycle 24:GB2007. http://dx.doi.org/10.1029/2009GB003618.

Larsen, S., Aanersen, T., Hessen, D.O., 2011. Climate change predicted to cause severe increase of organic carbon in lakes. Glob. Chang. Biol. 17, 1186–1192.

Leithold, E.L., Blair, N.E., Wegmann, K.W., 2016. Source-to-sink sedimentary systems and global carbon burial: a river runs through it. Earth Sci. Rev. 153, 30–42.

Liu, Y., Zhou, Y., Wu, W., 2015. Assessing the impact of population, income and technology on energy consumption and industrial pollutant emissions in China. Appl. Energy 155, 904–917.

Liu, H., Liu, W.G., 2016. n-Alkane distributions and concentrations in algae, submerged plants and terrestrial plants from the Qinghai-Tibetan Plateau. Org. Geochem. 99, 10–22.

Lu, Y.Q., 1999. Salicylate, hypochlorous acid salt spectrophotometry determination of ammonia nitrogen in water. J. Environ. Health 16 (5), 296–298 (Chinese with English abstract).

Lü, X., Zhai, S.K., 2006. Distributions and sources of organic biomarkers in surface sediments from the Changjiang (Yangtze River) Estuary, China. Cont. Shelf Res. 26, 1–14.

Mendonça, R., Kosten, S., Sobek, S., Cardoso, S.J., Figueiredo-Barros, M.P., Estrada, C.H., Roland, D.F., 2016. Organic carbon burial efficiency in a subtropical hydroelectric reservoir. Biogeosciences 13, 3331–3342.

Meyers, P.A., Ishiwatari, R., 1993. Lacustrine organic geochemistry-an overview of indicators of organic matter sources and diagenesis in lake sediments. Org. Geochem. 28, 867–900.

Meyers, P.A., 2003. Applications of organic geochemistry to paleolimnological reconstructions: a summary of examples from the Laurentian Great Lakes. Org. Geochem. 34, 261–289.

Ortiz, J.E., Díaz-Bautista, A., Aldasoro, J.J., Torres, T., Gallego, J.L.R., Moreno, L., Estébanez, B., 2011. N-alkan-2-ones in peat-forming plants from the Roñanzas ombrotrophic bog (Asturias, northern Spain). Org. Geochem. 42, 586–592.

Ortiz, J.E., Ángeles, G., Gallego, J.L.R., Sánchez-Palencia, Y., Urbanczyk, J., Torres, T., Domingo, L., Estébanez, B., 2016. Biomarkers and inorganic proxies in the paleoenvironmental reconstruction of mires: the importance of landscape in Las Conchas (Asturias, Northern Spain). Org. Geochem. 95, 41–54.

Pearson, A., Eglinton, T.I., 2000. The origin of n-alkanes in Santa Monica Basin surface sediment: a model based on compound-specific $\Delta^{14}C$ and $\delta^{13}C$ data. Org. Geochem. 31, 1103–1116.

Qian, J.L., Zhang, L.D., Yue, M.L., 1990. Persulfate digestion method for determination of total nitrogen and total phosphorus in soil. Soils 22 (5), 258–262 (Chinese with English abstract).

Quinton, J.N., Govers, G., Oost, K.V., Bardgett, R.D., 2010. The impact of agricultural soil erosion on biogeochemical cycling. Nat. Geosci. 3, 311–314.

Raymond, P.A., Hartmann, J., Lauerwald, R., Sobek, S., McDonald, C., Hoover, M., Butman, D., Striegl, R., Mayorga, E., Humborg, C., Kortelainen, P., Dürr, H., Meybeck, M., Ciais, P., Guth, P., 2013. Global carbon dioxide emissions from inland waters. Nature 503, 355–359.

Rao, Z.G., Jia, G.D., Qiang, M.R., Zhao, Y., 2014. Assessment of the difference between mid- and long chain compound specific δDn-alkanes values in lacustrine sediments as a paleoclimatic indicator. Org. Geochem. 76, 104–117.

Sanchez-Cabeza, J.A., Ruiz-Fernández, A.C., 2012. ^{210}Pb sediment radiochronology: an integrated formulation and classification of dating models. Geochim. Cosmochim. Acta 82, 183–200.

Silva, T.R., Lopes, S.R.P., Spörl, G., Knoppers, B.A., Azevedo, D.A., 2012. Source characterization using molecular distribution and stable carbon isotopic composition of n-alkanes in sediment cores from the tropical Mundaú-Manguaba estuarine-lagoon system. Brazil. Org. Geochem. 53, 25–33.

Simoneit, B.R.T., Cardoso, J.N., Robinson, N., 1990. An assessment of terrestrial higher molecular weight lipid compounds in aerosol particulate matter over the South Atlantic from about 30-70°S. Chemosphere 21, 1285–1301.

Sobek, S., Durisch-Kaiser, E., Zurbrugg, R., Wongfun, N., Wessels, M., Pasche, N., Wehrli, B., 2009. Organic carbon burial effciency in lake sediments controlled by oxygen exposure time and sediment source. Limnol. Oceanogr. 54, 2243–2254.

Sobek, S., Anderson, N.J., Bernasconi, S.M., Sontro, T.D., 2014. Low organic carbon burial efficiency in arctic lake sediments. J. Geophys. Res. Biogeosci. 119, 1231–1243.

Sojinu, O.S., Wang, J.Z., Sonibare, O.S., Zeng, E.Y., 2010. Polycyclic aromatic hydrocarbons in sediments and soils from oil exploration areas of the Niger Delta, Nigeria. J. Hazard Mater. 174, 641–647.

Stief, P., 2007. Enhanced exoenzyme activities in the presence of deposit-feeding *Chironomus riparius* larvae. Freshw. Biol. 52, 1807–1819.

Stout, S.A., Uhler, A.D., McCarthy, K.J., Emsbo-Mattingly, S., 2002. Chemical fingerprinting of hydrocarbons. In: Murphy, B.L., Morrison, R. (Eds.), Introduction to Environmental Forensics. Academic Press, Boston, pp. 137–260.

Tranvik, L.J., Downing, J.A., Cotner, J.B., Loiselle, S.A., Striegl, R.G., Ballatore, T.J., Dillon, P., Finlay, K., Fortino, K., Lesley, B.K., Kortelainen, P.L., Kutser, T., Larsen, S., Laurion, I., Leech, D.M., McCallister, S.L., McKnight, D.M., Melack, J.M., Overholt, E., Porter, J.A., Prairie, Y., Renwick, W.H., Roland, F., Sherman, B.S., Schindler, D.W., Sobek, S., Tremblay, A., Vanni, M.J., Verschoor, A.M., Wachenfeldt, E., Weyhenmeyer, G.A., 2009. Lakes and reservoirs as regulators of carbon cycling and climate. Limnol. Oceanogr. 54, 2298–2314.

Wang, P., Wu, W., Zhu, B., Wei, Y., 2013. Examining the impact factors of energy-related CO2 emissions using the STIRPAT model in Guangdong Province, China. Appl. Energy 106, 65–71.

Wang, J.Z., Nie, Y.F., Luo, X.L., Zeng, E.Y., 2008. Occurrence and phase distribution of polycyclic aromatic hydrocarbons in riverine runoff of the Pearl River Delta, China. Mar. Pollut. Bull. 57, 767–774.

Wang, Z.D., Fingas, M., 2005. Oil and Petroleum Product Fingerprinting Analysis by Gas Chromatographic Techniques. CRC Press, New York.

Watanabe, K., Kuwae, T., 2015. How organic carbon derived from multiple sources contributes to carbon sequestration processes in a shallow coastal system? Glob. Chang. Biol. 21, 2612–2623.

Wu, P.B., Gao, C., Chen, F.R., Yu, S.R., 2016. Response of organic carbon burial to trophic level changes in a shallow eutrophic lake in SE China. J. Environ. Sci. 46, 220–228.

Xie, S.C., Yi, Y., Huang, J.H., 2003. Lipid distribution in a subtropical southern China stalagmite as a record of soil ecosystem response to paleolimate change. Quaternary Sciences 60, 340–347.

Xiong, Y.Q., Wu, F.C., Fang, J.D., Wang, L.F., Li, Y., Liao, H.Q., 2010. Organic geochemical record of environmental changes in Lake Dianchi, China. J. Paleolimnol. 44, 217–231.

York, R., Rosa, E.A., Dietz, T., 2003. STIRPAT, IPAT and ImPACT: analytic tools for unpacking the driving forces of environmental impacts. Ecol. Econ. 46, 351–365.

Zhao, M., Dupont, L., Eglinton, G., Teece, M., 2003. Alkane and pollen reconstruction of terrestrialclimate and vegetation for N.W. Africa over the last 160 kyr. Org. Geochem. 34, 131–143.

Zhou, Y., Liu, Y.S., 2016. Does population have a larger impact on carbon dioxide emissions than income? Evidence from a cross-regional panel analysis in China. Appl. Energy 180, 800–809.

Zhou, Y., Liu, Y.S., Wu, W., Li, Y., 2015. Effects of rural-urban development transformation on energy consumption and CO_2 emissions: a regional analysis in China. Renew. Sust. Energ. Rev. 52, 863–875.

Zhou, Q.C., Zhang, Y.L., Lin, D.M., Shan, K., Luo, Y., Zhao, L., Tan, Z.W., Song, L.R., 2016. The relationships of meteorological factors and nutrient levels with phytoplankton biomass in a shallow eutrophic lake dominated by cyanobacteria, Lake Dianchi from 1991 to 2013. Environ. Sci. Pollut. Res. 23, 15616–15626.